

Thermally Induced Molecular Motion and Premelting in the Solid State of *n*-Hexatriacontane

Michael J. Stewart, William L. Jarrett, and Lon J. Mathias*

Department of Polymer Science, University of Southern Mississippi,
Hattiesburg, Mississippi 39406-0076

Rufina G. Alamo and Leo Mandelkern*

Department of Chemistry and Institute of Molecular Biophysics, Florida State University,
Tallahassee, Florida 32306

Received January 30, 1995; Revised Manuscript Received November 15, 1995[®]

ABSTRACT: A combination of differential scanning calorimetry and solid-state CP/MAS ¹³C NMR studies of pure *n*-C₃₆H₇₄ (hexatriacontane) were carried out to evaluate its thermal behavior in the solid state with increasing temperature. Three different modes of crystallization were used, and particular attention was given to the NMR behavior relative to the pseudohexagonal transition. Peak sharpening due to increased molecular motion and chemical shift changes characteristic of increasing populations of gauche conformations near the chain ends were observed below the pseudohexagonal transition. These observations confirm a gradual increase in the conformational mobility of segments near the crystal surface with increasing temperature. The interior methylenes, however, maintain their all-trans conformation up to the transition to the pseudohexagonal phase at 72.6–72.7 °C. The combination of techniques employed clearly confirmed the occurrence of premelting (defined as the disordering of chain-end segments) at ca. 15–20 °C below the melting point, depending on sample treatment.

Introduction

The *n*-alkanes exhibit a variety of different crystalline structures and transitions between those forms. This not only is true for the different alkanes but also occurs within a given species. The specifics of the transitions in a given molecule depend on the mode of crystallization. Another characteristic of the fusion of the *n*-alkanes is the disordering of the units in the end sequences at temperatures well below the melting temperature of the compound. As a consequence of this disruption, the planar array of end groups, typical of molecular crystals, is destroyed. We shall designate this process as premelting. It needs to be distinguished from other phenomena that have also been given the same terminology.¹ Direct evidence for this type of premelting has been demonstrated by solid-state NMR measurements^{2–6} and vibrational spectroscopy.^{7–11} In addition to these direct observations of premelting, there are a set of other experimental observations that are consistent with and most easily comprehended by this phenomenon.¹ These include, among others, thermodynamic properties, X-ray scattering, electron diffraction, lattice expansion, and neutron scattering. A summary of these results can be found in ref 1.

A particular crystal–crystal transition that is found in some of the *n*-alkanes is of special interest. In this case, either an orthorhombic or monoclinic crystal structure is cooperatively transformed to a pseudohexagonal structure, often termed “the rotator phase”.¹² The transition to the pseudohexagonal phase is only observed in odd carbon numbered chains between C₉H₂₀ and C₄₃H₈₈ and in even carbon numbered ones between C₂₂H₄₆ and C₄₀H₈₂. The NMR and vibrational spectroscopic studies that have been made in the pseudohexagonal phase demonstrate quite definitely that the end-group sequences are disordered in this state. These experimental data also suggest that the temperature for the onset of chain disordering of end sequences is

below the actual temperature for the transition to the hexagonal form. However, the experimental data are not definite on this point. If this were in fact the case, then the end-disordering process could serve as the precursor or “trigger” for the transition to the hexagonal phase. Since the experimental results are not clear on this important point, further studies to clarify this matter appear to be in order. Consequently, we report the results of a CP/MAS ¹³C NMR study as a function of temperature, accompanied by differential scanning calorimetric data, of *n*-hexatriacontane. This compound displays an established and well-defined pseudohexagonal transition. Samples crystallized by three different methods were studied. Small temperature increments were used in the vicinity of, and through, the transition regions.

Experimental Section

The *n*-hexatriacontane sample was purchased from Fluka and purified by recrystallization from a 4% butyl acetate solution. Mass spectra analysis of the recrystallized sample showed that no impurities were present with masses differing from that of *n*-hexatriacontane. (We wish to thank Prof. Alan G. Marshall of Florida State University for the mass spectra analysis.) Although the mass spectra cannot rule out isomeric impurities, the synthetic method normally used for making these compounds precludes this possibility. More importantly, no evidence was obtained from NMR indicating a branched site carbon. This method of purification was successfully used by Barnes¹³ to remove an impurity in a lower molecular weight alkane. In VanderHart's classic solid-state ¹³C NMR study of *n*-alkanes, the samples were purified either by recrystallization or by zone refining.¹⁴ There is the clear implication in this work that the same ¹³C NMR results are obtained by either purification method. The evidence cited above demonstrates the purity of our sample in terms of the physicochemical measurements of interest here.

Samples for evaluation were prepared using three crystallization procedures: (i) rapid crystallization from the pure melt; (ii) rapid crystallization from a propyl acetate solution; and (iii) slow crystallization from a propyl acetate solution. Treatment (i) was carried out either by melting the sample in an NMR rotor and transferring the rotor to an ice water bath

[®] Abstract published in *Advance ACS Abstracts*, May 15, 1996.

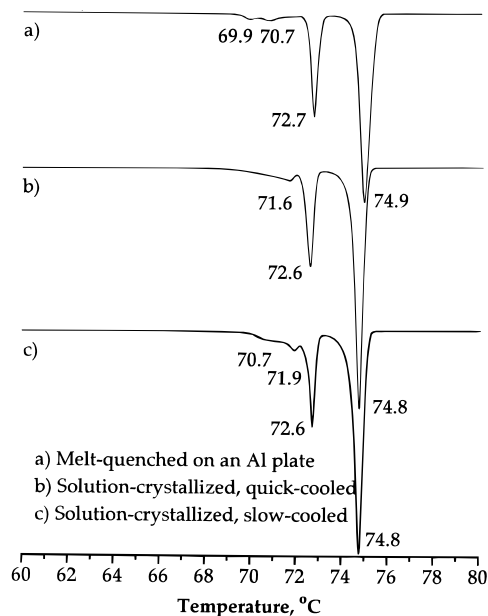


Figure 1. Thermograms of different sample treatments of hexatriacontane.

or by quenching from the melt onto an aluminum plate. Treatment (ii) involved dissolving the sample in propyl acetate and plunging the flask containing the solution into an ice water bath. In treatment (iii), after dissolution, heat was removed from the oil bath and stirring continued as the solution slowly cooled to room temperature. In both solution treatments, the resulting precipitate was collected, washed with water, and dried *in vacuo* at ambient temperature for more than 24 h.

DSC measurements were conducted on a TA Instruments Model 2920 thermal analyzer operating in conventional mode. The calorimeter was calibrated with indium. Samples were heated at 0.5 °C/min. Thermograms were processed on-line using a TA Instruments Thermal Analyst 2100 and off-line using Origin¹⁵ on a 486 microcomputer. Samples were sealed in hermetic pans, and all measurements were conducted under a nitrogen atmosphere.

Solid-state ^{13}C NMR spectroscopy was performed on a Bruker MSL-400 spectrometer operating at a field strength of 100.043 MHz for carbon. Carbon data were acquired using magic-angle spinning with cross-polarization (CP/MAS) and high-power proton decoupling (HPD) during signal acquisition. CP/MAS experiment times were shortened through the use of a flipback pulse (negative ^1H 90° pulse). ^{13}C chemical shift values were referenced to the upfield shift of adamantane at 300 K (29.5 ppm). The sample spinning rate was maintained at ~3000 Hz. A standard 4 mm double-air-bearing Bruker CP/MAS probe was used for the experiments. Drive and bearing pressures were held constant at 150 and 1160 mbar, respectively. A Bruker VT-1000 controller was used to regulate probe temperatures to ± 0.2 °C. The probe temperature readings were calibrated using ethylene glycol.¹⁶ Samples were allowed to equilibrate for 20–30 min at each temperature before spectral data were acquired. Data were processed off-line using SpectraCalc¹⁷ and SC NMR, a SpectraCalc Array Basic program written in-house for analyzing NMR data files on 486 microcomputers,¹⁸ and Origin.

Results and Discussion

DSC. The thermograms for samples generated by slow crystallization from propyl acetate (NQ), by rapid crystallization from propyl acetate (Q), and by rapid crystallization from the melt by quenching on an aluminum plate (M) are shown in Figure 1. These samples were analyzed at a 0.5 °C/min scan rate on the TA Instruments 2920 thermal analyzer. The NQ and M samples are similar in that they both show four distinct transitions: melting at 74.8–74.9 °C, the

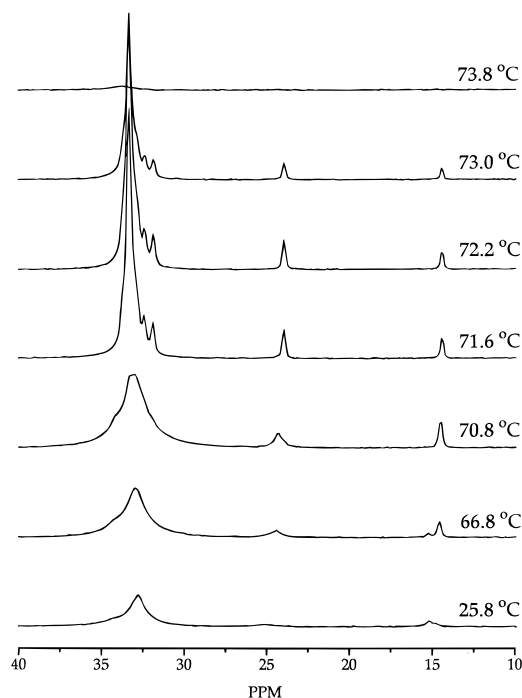


Figure 2. ^{13}C VT-CP/MAS NMR of melt-crystallized (sample M) $\text{C}_{36}\text{H}_{74}$.

pseudohexagonal (or “rotator phase”) transition at 72.6–72.7 °C, and two small endothermic transitions at 70.7 and 71.9 °C in the NQ sample and at 69.9 and 70.7 °C in the M sample. The Q sample shows three distinct transitions: melting at 74.8 °C, pseudohexagonal transition at 72.6 °C, and a broad low-temperature transition that has a peak at 71.6 °C. The highest overall transitional enthalpy (as measured by the total peak area for all the transitions) is displayed by the NQ sample (270.4 J/g). This is followed by the Q sample (269.5 J/g) and the M sample (250.2 J/g). Our thermograms in the temperature region of the “rotator phase” and the melting transition are identical, in terms of transition temperatures and endotherm shape, to that reported by Sullivan and Weeks.¹⁹ The latter investigators used both recrystallization and zone refining to purify their sample of *n*-hexatriacontane. The essential identity of results between the two works indicates the high purity of the sample studied in this work.

Low-temperature endothermic peaks representing the solid–solid transition from one monoclinic polymorphic form to another or from a monoclinic to an orthorhombic structure are commonly observed in *n*-alkanes.^{19,20} It has been established that very pure samples are required in order to observe the monoclinic form.²¹ Thus, our observation of the monoclinic form further attests to the high purity of the sample studied here. The thermogram in Figure 1a for the melt-crystallized sample is very similar to that reported by Möller *et al.*⁴ for melt-crystallized hexatriacontane as well as other reports in the literature for this compound.²⁰ The DSC thermograms in Figure 1 will serve as a guide in the analysis of the ^{13}C spectra.

^{13}C NMR. The ^{13}C solid-state NMR spectra of the three hexatriacontane samples that were studied are given in Figures 2–4. The features that are common to all these samples will be considered first.

The all-trans methylene peak (32.9 ppm) displays a slight narrowing with temperature as the pseudohexagonal transition is approached. Upon entering the pseudohexagonal phase, the peak suddenly narrows and

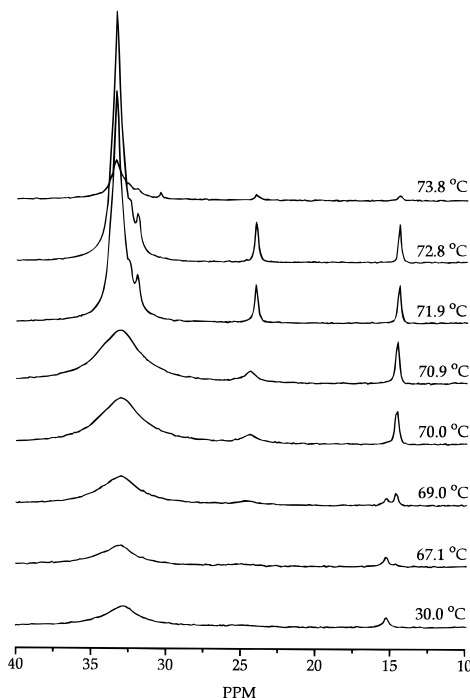


Figure 3. ^{13}C VT-CP/MAS NMR of quickly solution-crystallized (sample Q) $\text{C}_{36}\text{H}_{74}$.

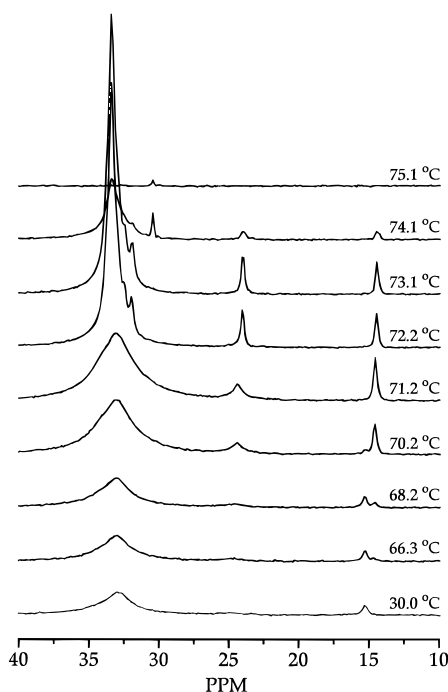


Figure 4. ^{13}C VT-CP/MAS NMR of slowly solution-crystallized (sample NQ) $\text{C}_{36}\text{H}_{74}$.

shoulder peaks are revealed on either side. These correspond to the γ , δ , and ϵ peaks (fourth, fifth, and sixth carbons from the end of the chain, respectively). The shoulders remain evident up to melting. Upon melting, all of the peaks in this region disappear. Cross-polarization remains strong at all temperatures below melting, indicating that the sample is still more rigid than in the molten state. Table 1 compares the CP/MAS chemical shift values obtained experimentally for the NQ, Q, and M samples with HPD/MAS chemical shift values published by Möller *et al.*⁴ The difference of ~ 1 ppm between Möller's⁴ values and the values in Table 1 is due to the use of an alternative chemical shift referencing technique.

As is indicated in Figures 2–4, noncooperative processes, in which carbon populations gradually move from one discrete environment to another, take place for the methyl carbons at temperatures below any of the transitions observed by DSC. For $\text{C}_{36}\text{H}_{74}$, the process involved is a transition from a crystal-bound methyl (15.2 ppm) to a γ -gauche deshielded methyl (14.4–14.8 ppm) which has been partially excluded from the crystal matrix. With increasing temperature, the 15.2 ppm peak gradually decreases as the 14.4 ppm peak increases in intensity. These processes are seen to occur over the broadest range of temperatures for the M sample (from room temperature up to 71 °C) and over the narrowest range for the NQ sample (from 66.3 to 70 °C). The presence of two distinct chemical environments for the methyl carbons is a strong indication of the disordering of chain-end sequences in the crystals. The closeness of the chemical shift of the upfield methyls in the surface-disordered phase (14.5–14.7 ppm) to the pseudohexagonal/melt chemical shift (14.4 ppm) is an indication of high mobility at temperatures significantly below the melt and of already having reached a state where the methyls experience virtually the same ratio of trans/gauche states as they do in the melt. If we assume that there is a linear correspondence between chemical shift and liquid- or melt-like behavior (based on a corresponding change in nuclear environment), then these methyls can be said to be 63–88% liquid-like or melted.

Figures 2–4 show quite clearly that the sharpness and/or intensity of the α -CH₂ peak begins to increase at temperatures below that of the transition to the pseudohexagonal phase. The sharpness and/or intensity of the α -CH₂ peak below the pseudohexagonal phase appears to be directly proportional to the amount of conformational disorder on the crystal surface. This peak is almost buried in the spectral noise for the NQ and Q samples. The M sample, on the other hand, displays a rather clear peak from room temperature up through the melt. This is consistent with greater disorder at the α -CH₂ position for this sample than for the other two. The same argument can be applied to the internal-CH₂ region (30–35 ppm).

We can now consider aspects of the spectra characteristic of each different mode of crystallization. The VT-CP/MAS NMR results (Figure 2) for the M sample show two methyl peaks from room temperature up to about 70 °C. The downfield crystal-entrained peak (15.2 ppm) slowly decreases in intensity and disappears completely before the pseudohexagonal transition. The upfield γ -gauche peak (14.8–14.4 ppm) slowly increases in intensity and remains apparent until melting. The presence of the γ -gauche CH₃ peak at room temperature is indicative of a high degree of end-group disordering for this sample at relatively low temperature.

The α -CH₂ peak (25.0 ppm) displays greater intensity and sharpness in the M sample than in the solution-crystallized samples at temperatures below the pseudohexagonal transition. This peak moves upfield with increasing temperature, from 25.1 ppm in the rigid crystalline phase to 24.4 ppm in the premelt to 24.0 ppm at the transition to the pseudohexagonal phase, and another shift to 23.3 ppm in the melt.²² This shift is a product of increasing γ -gauche interactions due to greater availability of gauche conformations at the lamellar surface. The smaller upfield shift of the α -CH₂ peak in this temperature region, as compared to the changes observed in the methyl carbon, is due to the

Table 1. Comparison of Experimental CP/MAS and Literature HPD/MAS ^{13}C Chemical Shift Values for $n\text{-C}_{36}\text{H}_{74}$ ^a

		internal -CH ₂ -	CH ₃	$\alpha\text{-CH}_2$	$\beta\text{-CH}_2$	$\gamma\text{-CH}_2$	$\delta\text{-CH}_2$	$\epsilon\text{-CH}_2$
ordered (monoclinic) crystal phase	Möller ^b	33.7	16.1	25.7	35.2			
	NQ ^c	32.9	15.2	25.1	34.3			
	Q	32.9	15.3	25.0	34.2			
	M	32.7	15.2/14.8 ^d	25.1	34.3			
surface-disordered crystal phase	Möller ^b	33.7	16.1/15.4 ^d	25.2	35.0			
	NQ ^c	33.0	15.2/14.5 ^d	24.6	34.2			
	Q	32.9	15.3/14.7 ^d	25.0	34.3			
	M	33.0	15.2/14.5 ^d	24.4	34.2			
pseudohexagonal phase	Möller ^b	34.2	15.2	24.8	34.5	32.7	33.2	33.8
	NQ	33.3	14.4	24.0	33.6	31.9	32.4	32.7
	Q	33.4	14.4	24.0	33.7	32.0	32.5	32.9
	M	33.3	14.4	24.0	33.7	31.9	32.4	32.9
melt	Möller ^b	31.2	15.2	24.0	33.4	30.7		
	NQ, Q, and M ^{c,e}	30.4	14.4	23.3	32.6	29.9		

^a NQ = slowly solution-crystallized; Q = quickly solution-crystallized; M = quickly melt-crystallized. ^b See ref 4 for chemical shift referencing procedure. ^c Referenced to upfield shift of adamantane at 300 K (29.5 ppm). ^d Two distinct chemical environments exist for these carbons; see text. ^e Melt chemical shifts obtained from HPD/MAS spectrum.

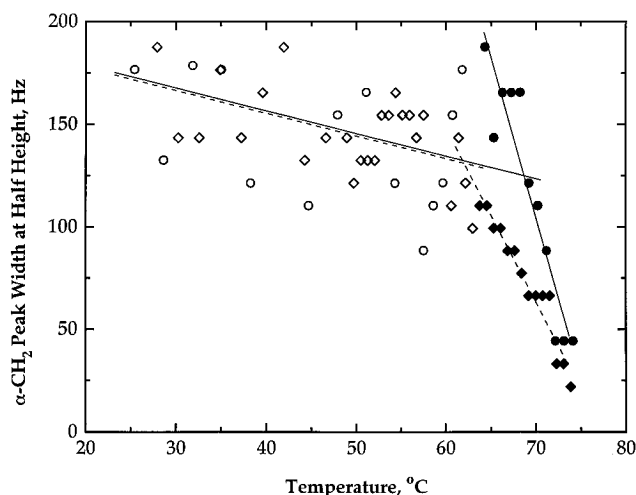


Figure 5. Peak width at half-height for the $\alpha\text{-CH}_2$ peak (24.0–25.1 ppm) of the M (○, ●) and NQ (◇, ◆) samples. Open symbols were used for the lower temperature linear regression, and filled symbols were used for the higher temperature regression. Regression lines for the M (---) and NQ (—) samples are also shown.

greater degree of lateral chain motion out of the crystal lamella that is necessary for this carbon to experience the γ -gauche effect.

Plots of $\alpha\text{-CH}_2$ peak width at half-height vs temperature were constructed to examine trends in line shape for each of the crystallization modes. The data for the melt-crystallized sample and the one slowly cooled from solution are given in Figure 5. Since the $\alpha\text{-CH}_2$ peak is very broad at low temperatures, accurate measurement of its width at half-height was difficult. Therefore, there is a large scattering of the data at temperatures below $\sim 68^\circ\text{C}$ for the NQ sample and below $\sim 62^\circ\text{C}$ for the M sample. These data points are plotted as open symbols in the figure. However, in the higher temperature range, represented by closed symbols in the figure, there is a very good correlation between the peak width at half-height and the temperature. The data for the two melt-crystallized samples, the M sample and a sample melt-quenched into liquid nitrogen, delineate a single straight line. The solution-crystallized samples Q and NQ fall on another, steeper straight line. The scattering of the data precludes any systematic discussion of the low-temperature region. However, an analysis can be made of the data in the high-temperature region. In this region, for both the melt- and solution-crystallized samples, the width of the $\alpha\text{-CH}_2$ peak narrows very

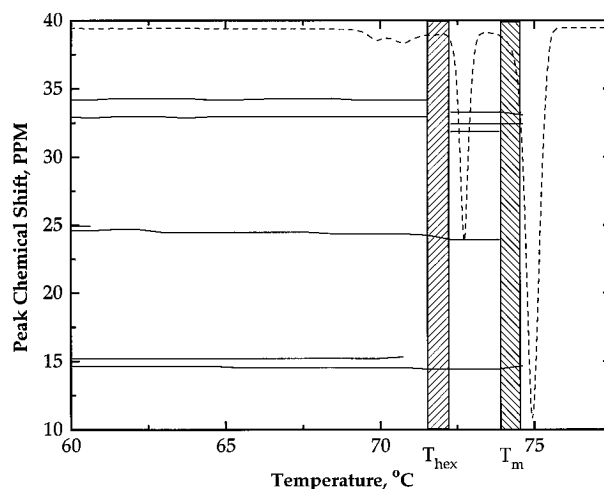


Figure 6. Correlation of changes in peak chemical shifts (solid lines) with thermal transitions (dashed line) for the M sample. Shaded areas represent ranges in which the NMR-observed pseudohexagonal and melting transitions occur.

rapidly with increasing temperature. The narrowing results from enhanced mobility of these carbons within the well-defined crystal lattice. The initial constraints on the motion of the $\alpha\text{-CH}_2$ carbons are reduced in this temperature region, and gauche conformations are adopted, consistent with the upfield shift and line narrowing. Figure 5 indicates that changes are very cooperative, beginning in a temperature interval of $60\text{--}65^\circ\text{C}$. This temperature range is well below the onset of the pseudohexagonal transition. Thus, the increased conformational disorder at the crystal surface apparently induces this transition as well as other solid–solid transitions in this and other n -alkanes.^{1,19,20} We should also note that in the higher temperature region the line widths of the solution-crystallized samples are significantly broader than those of the melt-crystallized samples. This reflects a decreased molecular mobility of the solution-crystallized materials, implying that they maintain a higher degree of order at a given temperature.

To better visualize the spectral shifts and to allow a direct comparison with the DSC endotherms, both types of measurements were overlaid in a single diagram. Figure 6 displays points for peaks from the variable-temperature ^{13}C NMR data overlaid with an enlarged section of the DSC thermogram for the M sample. Most of the chemical shift changes in the NMR data can be

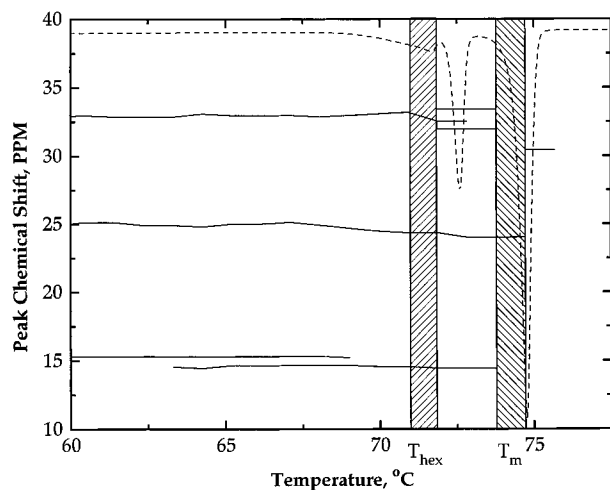


Figure 7. Correlation of changes in peak chemical shifts (solid lines) with thermal transitions (dashed line) for the Q sample. Shaded areas represent ranges in which the NMR-observed pseudo-hexagonal and melting transitions occur.

discerned in the temperature region of the low-temperature endotherm and continue into the pseudo-hexagonal phase. The onset of the 69.9 °C endotherm correlates with a slight upfield shift in the α -CH₂ peak at 24.4 ppm and a corresponding upfield shift in the methyl peak at 14.5 ppm. The second low-temperature endotherm corresponds to a slight downfield shift and then disappearance of the methyl peak at 15.2 ppm.

Quickly cooling the propyl acetate solution of *n*-C₃₆H₇₄ has been reported to yield the orthorhombic modification.^{20,21} The spectra for this sample (Figure 3) show that it has much less chain-end disorder than the M sample. This is evidenced by the delayed appearance (at ~63 °C) and lower relative intensity of the upfield (disordered) methyl peak (14.4 ppm). The presence of this 14.4 ppm peak indicates that some crystalline or surface disorder is present or that the sample is undergoing a crystal-surface "roughening" during the heating cycle. Both of the solution-crystallized samples display significant disordered-methyl peak intensity at 14.4 ppm above 60 °C, indicating that the samples maintain a degree of crystalline uniformity and surface rigidity over a wider temperature interval than the melt-crystallized sample. Therefore, the premelting temperature is greater than that of the M sample.

As pointed out above, the two solution samples also show broader peaks for the α -CH₂ (and also the internal CH₂) than the M sample. This is due to the conformational-averaging effect of increased molecular motion in the M sample homogenizing the chemical shifts somewhat more than in the Q and NQ samples. This observation is in agreement with the expectation that the crystal will be better organized when formed from solution.

The DSC thermogram for the Q sample overlaid with chemical shifts for the VT-NMR spectral peaks is given in Figure 7. The later onset, ca. 63 °C, of the gauche-disordered methyl peak, as compared to below 30 °C for the melt-crystallized sample (see Figure 6), is in accord with a crystal that has fewer surface imperfections. The crystalline methyl peak at 15.2 ppm disappears at a temperature that corresponds to the onset of the low-temperature endotherm at ~69 °C. This endotherm is associated with solid–solid phase transitions.^{12a} However, conformational disorder at the crystal surface is occurring at a lower temperature, as evidenced by the

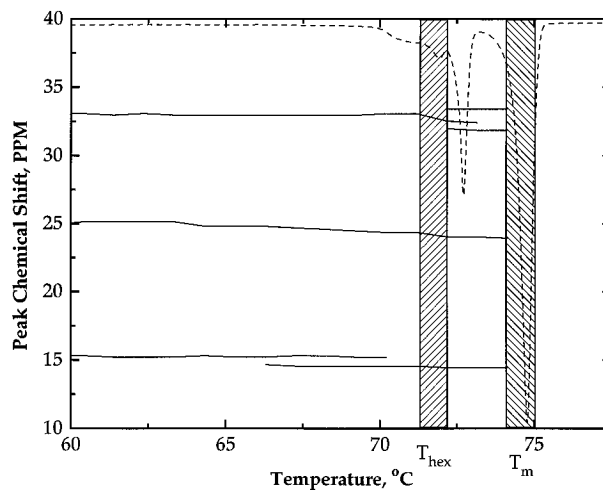


Figure 8. Correlation of changes in peak chemical shifts (solid lines) with thermal transitions (dashed line) for the NQ sample. Shaded areas represent ranges in which the NMR-observed pseudo-hexagonal and melting transitions occur.

appearance of the γ -gauche methyl peak at ~63 °C and the well-defined cooperative narrowing of the α -CH₂ peak at approximately 64 °C (Figure 5).

The DSC/NMR overlay for the slowly solution-crystallized sample, NQ, is given in Figure 8. The 14.4 ppm γ -gauche methyl peak appears at about 67 °C. This temperature is higher than the corresponding ones for the rapidly crystallized solution sample and the melt-crystallized sample. The sudden upfield shift of the α -CH₂ resonance at this temperature and the concomitant narrowing of the line width are also related to the development of gauche conformations. The internal-CH₂ resonance remains relatively unchanged up to a temperature corresponding to the pseudo-hexagonal transition in this sample, as well as the others studied.

From the behavior of the 14.4 ppm methyl peak, we can conclude that the NQ sample possesses the highest degree of order from among the three samples studied. On the other hand, the observation of this peak in the M sample at the lowest temperatures studied indicates that a certain amount of gauche conformation is present under these conditions. The amount increases with increasing temperature. At a given temperature, the end-sequence disorder at the crystal surface of the M sample will be greater than that of the Q or NQ samples. As a consequence, the small, low-temperature endotherm characteristic of a solid–solid transition appears more defined and at a lower temperature, 69.8 °C, than that for the solution-crystallized samples at about 71 °C.

Conclusions

Premelting, as defined by the disordering of chain-end sequences and the accompanying enhancement of segmental motion, was clearly observed in all the *n*-hexatriacontane samples at temperatures that were well below the transition to the pseudo-hexagonal phase. These results thus complement and substantiate in more detail the previous vibrational spectroscopic studies.^{7,8} These changes increase rapidly and continue through the transition to melting. The premelting temperature is related to the initial surface disorder of the system. The ranking of the degree of disorder, M > Q > NQ, was determined by the temperature at which the gauche methyl peak appeared. Solution-crystallized

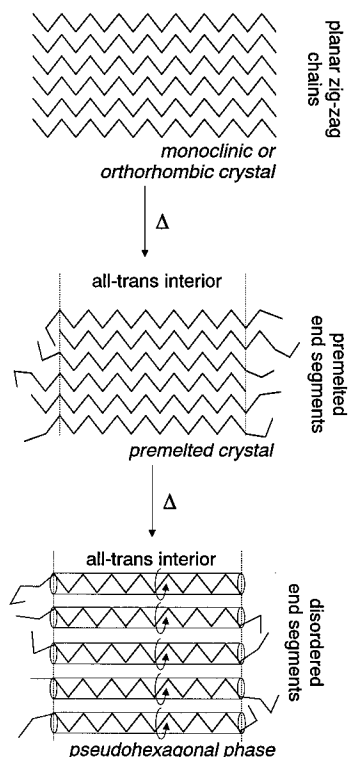


Figure 9. Schematic representation of submelting molecular motions in $C_{36}H_{74}$.

samples also displayed much broader α -CH₂ peaks than the melt-crystallized samples did at a given temperature. The disordering of the chain end-sequences is a precursor to the pseudo-hexagonal transition and appears to be the reason for the occurrence of this phase. The theoretical implications of these results still need to be investigated. The relaxations that occur in the pseudo-hexagonal phase cannot be attributed solely to the rotation of a rigid molecule. Contributions from the motion of the disordered end sequences must clearly be taken into account.

A schematic representation of the conclusions derived from these results is given in Figure 9. One starts, initially, with a set of completely ordered, planar zigzag chains that are in either orthorhombic or monoclinic packing with chain ends in register. Upon heating, disordering of the end sequences takes place. The temperature of this disordering depends on the mode of crystallization. Upon further heating, the transition to the pseudo-hexagonal phase takes place with the end disorder being maintained.

The HPD MAS ¹³C NMR data of Möller *et al.* on melt-crystallized hexatriacontane fits into the pattern observed here. Similar chemical shifts were observed over corresponding temperature and structural regions. We have, however, studied a larger temperature range and different modes of crystallization. This has allowed for a more detailed analysis and a more definitive conclusion with respect to the onset of premelting.

Acknowledgment. The work at the University of Southern Mississippi was supported in part by the Office of Naval Research, including a National Defense Science and Engineering Graduate Fellowship for one of the authors (M.J.S.). The work at the Florida State University was supported by the National Science Foundation Polymers Program (Grant DMR94-19508). This support is publicly acknowledged.

References and Notes

- (1) Mandelkern, L.; Alamo, R. G.; Dorset, D. L. *Acta Chim. Hung.* **1993**, *130*, 415.
- (2) Jarrett, W. L.; Mathias, L. J.; Alamo, R. G.; Mandelkern, L.; Dorset, D. *J. Am. Chem. Soc.* **1992**, *25*, 3468.
- (3) Ishikawa, S.; Kurosu, H.; Ando, I. *J. Mol. Struct.* **1991**, *248*, 361.
- (4) Möller, M.; Cantow, H.-J.; Drotloff, H.; Emeis, D.; Lee, K.-S.; Wegner, G. *Makromol. Chem.* **1986**, *187*, 1237.
- (5) VanderHart, D. L. *J. Magn. Reson.* **1981**, *44*, 117.
- (6) Stohrer, M.; Noack, F. *J. Chem. Phys.* **1977**, *67*, 3729.
- (7) Maroncelli, M.; Strauss, H. L.; Snyder, R. G. *J. Chem. Phys.* **1985**, *82*, 2811.
- (8) Kim, Y.; Strauss, H. L.; Snyder, R. G. *J. Phys. Chem.* **1989**, *93*, 7520.
- (9) Royaud, I. A. M.; Hendra, P. J.; Maddams, W.; Passingham, C.; Willis, H. A. *J. Mol. Struct.* **1990**, *239*, 83.
- (10) Zerbi, G.; Magni, R.; Gussoni, M.; Moritz, K. H.; Bigotto, A.; Dirlikov, S. *J. Chem. Phys.* **1981**, *75*, 3175.
- (11) Ewen, B.; Fischer, E. W.; Piesczek, W.; Strobl, G. *J. Chem. Phys.* **1974**, *61*, 5265.
- (12) (a) Muller, A. *Proc. R. Soc. London* **1930**, *A127*, 417. (b) Muller, A. *Proc. R. Soc. London* **1937**, *A158*, 403. (c) Muller, A. *Proc. R. Soc. London* **1940**, *A174*, 137.
- (13) Barnes, J. D. *J. Chem. Phys.* **1973**, *58*, 5193.
- (14) VanderHart, D. L. *J. Magn. Reson.* **1981**, *44*, 117.
- (15) MicroCal, Inc., 22 Industrial Dr. East, Northampton, MA 01060.
- (16) English, A. *J. Magn. Reson.* **1984**, *57*, 491.
- (17) Galactic Industries Corp., 395 Main St., Salem, NH 03079.
- (18) Casey, P. K.; Jarrett, W. L.; Mathias, L. *J. Am. Lab.* **1991**, October, 40.
- (19) Sullivan, P. V.; Weeks, J. J. *Res. Natl. Bur. Stand.* **1970**, *74A*, 203.
- (20) Takamizawa, K.; Ogawa, Y.; Ogawa, T. *Polym. J.* **1982**, *14*, 441.
- (21) Teare, P. W. *Acta Crystallogr.* **1959**, *12*, 294.
- (22) Melt chemical shifts taken from an HPD/MAS spectrum. The sample was allowed to reach equilibrium at 74.9 °C before spectral acquisition.

MA950107K